Cellular Signalling 60 (2019) 81–90

Contents lists available at ScienceDirect

Cellular Signalling

journal homepage: www.elsevier.com/locate/cellsig

Lysophosphatidic acid induces integrin β6 expression in human oral squamous cell carcinomas cells via LPAR1 coupling to $G\alpha_i$ and downstream SMAD3 and ETS-1 activation

Mingyan Xu[a,1], Hao Yin[b,1], Yihuang Cai[a], Wenxia Huang[a], Qing Ji[a], Fan Liu[b], Songlin Shi[b], Xiaoling Deng[b,*]

[a] Engineering Research Center of Fujian University for Stomatological Biomaterials, Department of Stomatology and Affiliated Stomatological Hospital of Xiamen Medical College, Fujian, China
[b] Cancer Research Center, School of Medicine, Xiamen University, Xiamen, Fujian, China

ARTICLE INFO

Keywords:
Integrin beta-6
Lysophosphatidic acid
Oral cancer
Gene expression regulation
G protein coupled receptor

ABSTRACT

Integrin β6 (ITGB6), an epithelial-specific integrin, is upregulated in oral squamous cell carcinomas (OSCC) and is associated with progression and metastasis of OSCC. Lysophosphatidic acid (LPA), an important bioactive phospholipid present in saliva, has also been related to OSCC cell migration and invasiveness. LPA exerts its biological effects through signal transduction pathways that ultimately regulate gene expression. However, it is unclear whether LPA signaling is involved in *ITGB6* upregulation in OSCC. Therefore, the aim of the current study was to investigate the role of LPA in the regulation of *ITGB6* expression in OSCC cells, and to delineate the molecular signaling pathways involved. Using SAS and HSC-3 OSCC cell lines, we found that LPA increases *ITGB6* mRNA expression without affecting mRNA stability, suggesting that LPA acts by regulating *ITGB6* gene transcription. In addition, we show that LPA stimulation increases phosphorylation and binding of the transcription factors SMAD3 and ETS-1 to the *ITGB6* promoter resulting in *ITGB6* active transcription. Finally, we demonstrate that LPA-induced *ITGB6* expression is mediated via the LPA receptors 1 (LPAR1) coupling to $G\alpha_i$. Our findings provide insights into the molecular mechanism underlying *ITGB6* overexpression in OSCC and may have important implications for therapeutic purposes.

1. Introduction

Oral squamous cell carcinoma (OSCC) is a malignancy of the oral cavity squamous epithelium. Despite improvements in therapeutic strategies, OSCC remains the sixth most common cancer worldwide, and the prognosis for patients remains poor [1]. This may partially be explained by its aggressive growth pattern, high degree of invasion to surrounding tissues, and cervical lymph node metastasis [2]. Cancer invasion and metastasis are controlled by several mechanisms that involve many biologically active substances, including integrins, which are present in the cancer microenvironment and play important roles in cancer progression [3].

Integrins are heterodimeric transmembrane proteins consisting of an α and a β subunit [4]. In mammals, there are 18 α and 8 β subunits that noncovalently associate to form 24 different integrins expressed in specific repertoires in particular tissues [5]. The integrin β6 (ITGB6) partners with the integrin αv forming the αvβ6 heterodimer. ITGB6 is an epithelial-specific integrin that is not expressed, or at very low levels, in normal adult epithelia, but which is highly upregulated in a wide range of tumors including OSCC [6,7]. Several studies have found that *ITGB6* expression promotes keratinocyte and OSCC cells migration and invasion [8]. In addition, *ITGB6* expression levels have been associated with clinical outcomes and prognostic in OSCC [9]. These observations suggest that ITGB6 plays an important role in the development of OSCC, highlighting the need to understand the molecular mechanisms that lead to an increased *ITGB6* expression in OSCC.

Abbreviations: ITGB6, Integrin β6; OSCC, Oral squamous cell carcinoma; LPA, Lysophosphatidic acid; STAT3, Signal transducer and activator of transcription 3; C/EBPα, CCAAT/enhancer-binding protein α; ETS-1, Avian erythroblastosis virus E26 (v-ets) oncogene homolog-1; AP-1, Activator protein 1; SMAD3, Mothers against decapentaplegic homolog 3; GPCR, G-protein-coupled receptor; LPAR, Lysophosphatidic acid receptor

* Corresponding author at: Cancer Research Center, School of Medicine, Xiamen University, Xiangan South Road, Xiamen, Fujian 361102, China.
E-mail address: xiaolingdeng@xmu.edu.cn (X. Deng).

[1] Equal contribution.

https://doi.org/10.1016/j.cellsig.2019.04.008
Received 29 December 2018; Received in revised form 27 March 2019; Accepted 14 April 2019
Available online 15 April 2019
0898-6568/

Several transcription factors have been found to be involved in the regulation of *ITGB6* expression. For instance, we previously demonstrated that the signal transducer and activator of transcription 3 (STAT3) and C/EBPα are involved in the regulation of *ITGB6* basal expression [10], whereas JunB and CBP-mediated histone hyperacetylation are responsible for TGF-β1-induced *ITGB6* transcription in OSCC cells [11]. Additionally, the transcription factor ETS-1 has been involved in *ITGB6* transcriptional activation in HEK293 cells [12], whereas SMAD3 and AP-1 have been found to mediate TGF-β1-induced *ITGB6* expression in bile duct epithelial cells [13]. However, it is not clear how external stimuli, such as lipid mediators, promote *ITGB6* transcription in OSCC cells.

Lysophosphatidic acid (LPA) is a bioactive phospholipid that plays a pivotal role in a great range of physiological functions and pathological conditions including cancer [14]. LPA concentration has been found to be significantly high in the plasma of patients with ovarian and other gynecologic cancers, suggesting that LPA could be used as a biomarker in these cancers [15]. LPA is also abundant in saliva [16], where it has been found to be involved in OSCC tumorigenesis by stimulating cell migration, invasion and metastasis [17,18]. LPA exerts its effects by binding to its cognate G-protein-coupled receptor (GPCR). So far, six types of LPA receptors have been identified (LPAR1 to LPAR6), including the high-affinity LPA receptors LPAR1–3 [19]. Increasing evidence shows that LPARs participate in LPA-induced cellular effects in OSCC and head and neck squamous cell carcinoma (HNSCC) [17], suggesting that LPA and the downstream signaling pathways are important in OSCC carcinogenesis. We previously reported that LPA can induce αvβ6-mediated TGF-β activation via LPAR2 coupling to a $G\alpha_q$-mediated RhoA activation pathway in normal human bronchial epithelial cells [20]. However, the effect of LPA signaling on *ITGB6* overexpression in OSCC remains unclear.

The aim of the current study was to investigate the role of LPA in *ITGB6* upregulation in OSCC cells and to delineate the molecular signaling pathways involved.

2. Materials and methods

2.1. Cell culture

The human OSCC cell lines SAS and HSC-3 were purchased from the Japanese Collection of Research Bioresources (JCRB) Cell Bank. Cells were cultured in high-glucose Dulbecco's modified Eagle's medium (DMEM, Gibco BRL) supplemented with 10% fetal bovine serum (FBS, Gibco BRL), 100 U/ml penicillin and 0.1 mg/ml streptomycin, at 37 °C in a 5% CO_2 incubator.

2.2. Lysophosphatidic acid treatment

Oleoyl-l-α-lysophosphatidic acid sodium salt was purchased from Sigma (CAS NUMBER:22556-62-3) and was resuspended in phosphate-buffered saline (PBS), pH 7.2, up to 1 mM in the presence of 5% (*w/v*) bovine serum albumin (BSA), and it was directly added into the cell culture medium to a final concentration of 10 μM. All experiments involving LPA treatment were performed after serum starvation for 24 h.

2.3. RNA isolation and quantitative real-time PCR

Total RNAs were isolated from cells using General RNA Extraction Kit (Dongsheng Biotech, Guangzhou, China) according to the manufacturer's protocol and reverse transcribed with FastQuant RT Kit (TIANGEN BIOTECH, Beijing, China). Quantitative real-time RT-PCR (qRT-PCR) was performed using a SuperReal PreMix Kit (TIANGEN BIOTECH, Beijing, China) on an ABI StepOne system (ABI). The relative mRNA expression was calculated using the $2^{-\Delta\Delta Ct}$ method [21]. Ct data were normalized to the internal standard *β2-M*. The primers used for qRT-PCR are listed in Table 1. PCR was carried out by using PCR MIX (Dongsheng Biotech, Guangzhou, China).

Table 1
Primer sequences for quantitative RT-PCR.

Gene	Orientation	Sequences
ITGB6 F	5′–3′	GCAAGCTGCTGTGTGTAAGGAA
ITGB6 R	5′–3′	CTTGGGTTACAGCGAAGATCAA
SMAD3 F	5′–3′	GGTGCTCCATCTCCTACTACG
SMAD3 R	5′–3′	CGCCTCTTCCGATGTGTCT
ETS-1 F	5′–3′	CGCTATACCTCGGATTACTT
ETS-1 R	5′–3′	CTGATAGGACTCTGTGATGAA
LPAR1-F	5′–3′	ATCTATGTCAACCGCCGCTTCC
LPAR1-R	5′–3′	CCGTCAGGCTGGTGTCAATGAG
LPAR2-F	5′–3′	ACGCTCAGCCTGGTCAAGACT
LPAR2-R	5′–3′	GCATCTCAGCATCTCGGCAAGA
LPAR3-F	5′–3′	GCTGCTCAACTCCGTCGTGAAC
LPAR3-R	5′–3′	TGCCTGTGTCACTCCTGCTGAG
LPAR4-F	5′–3′	TCCTAGTCCTCAGTGGCGGTAT
LPAR4-R	5′–3′	CAGGCTTGCGAAGAGTTCTCAG
LPAR5-F	5′–3′	CTAGCCCTCTGGGTCTTCCT
LPAR5-R	5′–3′	CAGTGGTGCAGTGCGTAGTA
LPAR6-F	5′–3′	TCAGTAGTGGCAGCAGTAAGGA
LPAR6-R	5′–3′	TCAGGCAGCAGATTCATTGTCA
β2-M F	5′–3′	AATCCAAATGCGGCATCT
β2-M R	5′–3′	GAGTATGCCTGCCGTGTG

2.4. Construction of human ITGB6 promoter reporter plasmids

A series of 5′-deletion fragments of the human *ITGB6* promoter were cloned into the pGL2-basic firefly luciferase vector (Promega, Guangzhou, China) as previously described [10], resulting in the reporter vectors pGL2-B6(−909/+208), pGL2-B6(−421/+208), pGL2-B6(−150/+208), pGL2-B6(−3/+208), and pGL2-B6(−150/+22). Site-directed mutagenesis to inactivate the individual transcription factor potential binding sites in the *ITGB6* promoter was performed by the overlapping PCR-based approach [22]. The resulting reporter vectors pGL2-B6-M-ETS-1, pGL2-B6-M-SMAD3, pGL2-B6-ETS-1/SMAD3 contain the binding sites ETS-1, SMAD3, and both ETS-1 and SMAD3 mutated, respectively. The primers used are listed in Table 2.

2.5. Transient transfection

For promoter activity analysis, SAS cells seeded in 96-well plates ($4–5 \times 10^4$ cells/well) were transfected with 100 ng of plasmid (combined with 0.25 ng of pRL-TK) using METAFECTENE® EASY (Biontex, Germany) according to the manufacturer's protocol. Cells were harvested 48 h post-transfection.

2.6. RNA interference

RNA interference (RNAi) was performed using small interfering RNA duplex (siRNA) directed against the mRNAs of *SMAD3*, *ETS1*, *LPAR1, LPAR3* as well as a scrambled siRNA as a negative control. The siRNAs were obtained from Invitrogen Corporation and the sequences are described in Table 3. SAS cells were seeded in 6-well plates ($3–4 \times 10^5$ cells/well) and transfected with 150 pmol of siRNA using

Table 2
Primers for site-directed mutagenesis.

Primers	Orientation	Sequences
pGL2-B6-M-SMAD3 F	5′–3′	AAACACAGCTTT***GAG***GCTTTACCTGTCC
pGL2-B6-M-SMAD3 R	5′–3′	GGACAGGTAAAGC***CTC***AAAGCTGTGTTT
pGL2-B6-M-ETS-1 F	5′–3′	TGTACACCTGCC***GG***CCTTATAAGGAGAA
pGL2-B6-M-ETS-1 R	5′–3′	TTCTCCTTATAAGG***CC***GGCAGGTGTACA
B6 (−150) F	5′–3′	CGGGGTACCTAGGATGCAGAGAGACTCAT
B6 (+22) R	5′–3′	CCGCTCGAGAACAGAGGCTACCTGGAC

Mutation sites are bold and underlined.

Table 3
Sequences of siRNAs.

Gene	Orientation	Sense sequences
SMAD3	5′–3′	GGAGAAAUGGUGCGAGAAGTT
ETS-1	5′–3′	ACUUGCUACCAUCCCGUACTT
LPA1	5′–3′	GAAAUGAGCGCCACCUUUA
LPA3	5′–3′	CAGCAGGAGTTACCTTGTT

METAFECTENE® SI according to the manufacturer's protocol. Cells were harvested 24 h post-transfection for qRT-PCR and 72 h post-transfection for western blotting. Gene knockdown by RNAi was assessed by measuring the expression of the target genes by qRT-PCR and immunoblot.

2.7. Dual luciferase reporter assay

Firefly and *Renilla* luciferase activities were determined using the Dual-luciferase reporter assay system (Promega) and a Lumat LB9507 luminometer (Berthold). Firefly luciferase activity was normalized to *Renilla* luciferase readings in each well. Each experiment was conducted at least three times in triplicate.

2.8. Chromatin immunoprecipitation (ChIP) assay

ChIP was used to analyze binding of transcriptional factors to the *ITGB6* promoter in vivo as previously described [23]. After LPA-induction for 1 h, 1×10^7 SAS cells were treated with 1% formaldehyde for 10 min at 25 °C to cross-link the proteins to the DNA. This was followed by a 5 min treatment with glycine solution (125 mM final concentration) at room temperature to quench the formaldehyde. The

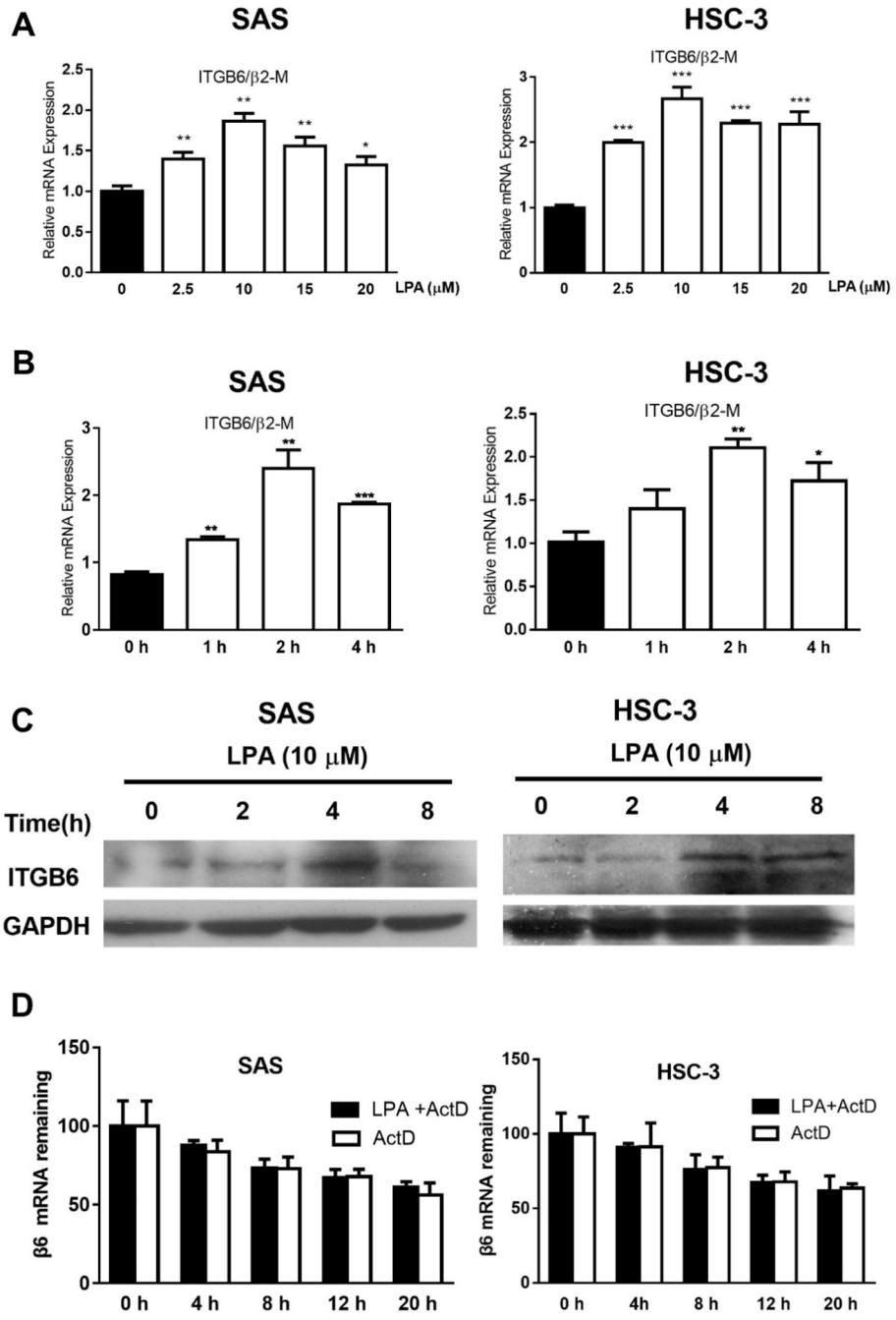

Fig. 1. LPA induces ITGB6 transcription in human OSCC cells. Serum-deprived confluent cells (SAS and HSC-3) were exposed to LPA for 2 h at (A) indicated concentrations (0, 2.5, 10, 15, or 20 μM) or (B) 10 μM LPA for different durations (0, 2, 4, or 8 h). Total RNA was then isolated, and *ITGB6* mRNA levels were assessed by qRT-PCR. Data are expressed as fold change relative to time zero or unstimulated cells after normalization to β2-M mRNA. $*p < .05$, $**p < .01$, $***p < 0.001$. (C) Serum-deprived confluent cells (SAS and HSC-3) were exposed to 10 μM LPA for different durations (0, 2, 4, or 8 h), and total cell lysates were then prepared for western blotting using specific anti-ITGB6 antibody. GAPDH was used as a loading control. (D) Effect of LPA on *ITGB6* mRNA stability. Confluent and serum-deprived cells were incubated with the general transcription inhibitor ActD (5 μg/ml), or ActD and LPA (10 μM) in combination for the indicated times. Total RNA was then isolated, and the mRNA levels of *ITGB6* and the internal control β2-M were determined by qRT-PCR. The results are calculated as the percent change in the ratio relative compared to the value at 0 h, before ActD treatment. Data are the mean ± SEM of three separate experiments performed in triplicate. $*p < 0.05$, $**p < .01$, $***p < .001$, compared with the medium control.

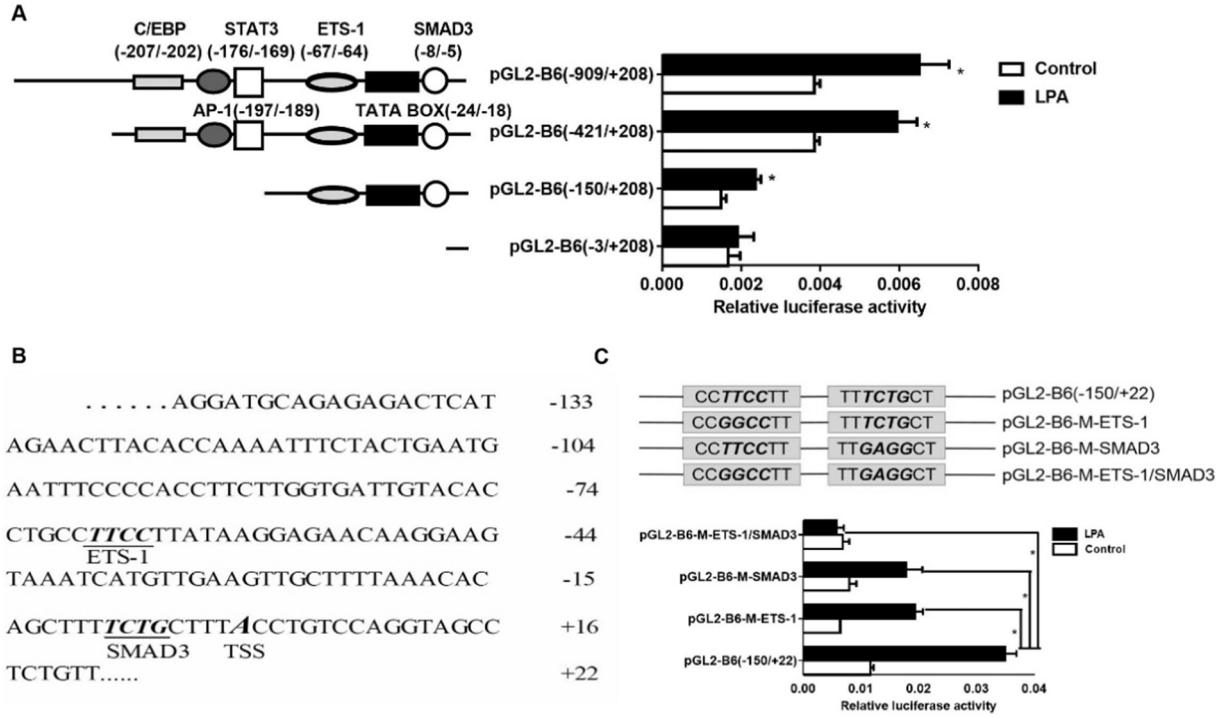

Fig. 2. Identification of *cis*-acting elements in the human *ITGB6* promoter responsible for LPA-induced *ITGB6* transcription. (A) Effect of LPA on *ITGB6* promoter activity in OSCC cells. SAS cells were transiently transfected with the *ITGB6* luciferase reporter constructs pGL2-B6(−909/+208), pGL2-B6(−421/+208), pGL2-B6(−150/+208), and pGL2-B6(+3/+208), followed by stimulation with LPA (10 μM) for 8 h. A diagram representing the *ITGB6* promoter region included in each reporter construct and the promoter elements that it contains is shown to the left, next to the corresponding reporter construct. The luciferase values are expressed as fold stimulation of the parent promoter-less vector pGL2-Basic, which was set to 1, and data are the mean ± SEM of three separate experiments performed in triplicate. *$p < .05$, compared with the medium control. (B) Nucleotide sequence of the human *ITGB6* promoter depicting the positions of the predicted ETS-1 and SMAD3 binding sites (underlined) and the transcriptional starting site (TSS). (C) Luciferase activity in SAS cells transfected with the reporter constructs pGL2-B6-M-ETS-1, pGL2-B6-M-SMAD3, and pGL2-B6-ETS-1/SMAD3 (with the predicted ETS-1, SMAD3, and both ETS-1 and SMAD3 binding sites mutated, respectively), or the wild-type construct pGL2-B6(−150/+22), following stimulation with LPA (10 μM) for 8 h. A diagram showing the sequence of the ETS-1 and SMAD3 binding sites in each of the reporter constructs used is shown at the top of panel c. *$p < 0.05$, compared with the medium control.

cells were then harvested, resuspended in 1% (*w/v*) SDS-lysis buffer, and sonicated (Sonifier Cell disruptor 350, Branson Sonic Power Co, MA) at 30% maximum power in three 15-s cycles with 30-s cooling intervals. The supernatant, containing the chromatin, was collected and diluted 10 folds in RIPA buffer (0.05 M Tris HCl, 150 mM NaCl, 1% NP-40, 1% sodium deoxycholate, 0.1% SDS) supplemented with protease inhibitor cocktail and phenylmethyl sulfonylfluoride, followed by overnight incubation at 4 °C with protein G agarose beads and 2 μg of the specific antibody or normal rabbit IgG as the negative control. Finally, the immunoprecipitates were washed, the antibody-protein-DNA complex was eluted from the beads, the cross-links were reversed, and the purified ChIP products were analyzed by qRT-PCR with primers F 5′-GCAGAGAGACTCATAGAACTT-3′ and R 5′-AACAGAGGCTACCTG GAC-3′.

2.9. Western blotting

Proteins isolated in RIPA buffer containing a cocktail of protease inhibitors (Sigma) were separated by sodium dodecyl sulfate-polyacrylamide gel electrophoresis (SDS-PAGE) and transferred to a nitrocellulose membrane. The membrane was blocked with non-fat milk followed by overnight incubation at 4 °C with anti-ITGB6 (Merck), anti-SMAD3 (CST), anti-ETS-1 (Santa Cruz), anti-p-SMAD3 (CST), anti-p-ETS-1(Thr38), anti-β-actin (Santa Cruz), and anti-GAPDH (Good Here, Hangzhou, China) antibodies. After incubation with a peroxidase-conjugated goat anti-rabbit or anti-mouse IgG, protein bands were visualized using Western Bright ECL (Advansta). Positive bands were semi-quantified by densitometric analysis using ImageJ software.

2.10. Cytotoxicity assay

SAS cells were plated at 1×10^4 cells/well in 96-well plates and treated with 0, 25, 50, 100, or 200 ng/ml pertussis toxin (PTX) for 24 h. Cell viability was subsequently determined using a Cell Counting Kit (CCK)-8 (Dojindo, Kumamoto Japan), according to the manufacturer's instructions, and the absorbance was measured at 450 nm on an Infinite F50 microplate reader (Tecan, Männedorf, Switzerland). Each experiment was carried out in quadruplicate for each condition, and the experiment was repeated three times independently.

2.11. Statistical analysis

All data are presented as mean ± SEM. The data were analyzed by two-tailed Student *t*-test, and $p < 0.05$ was considered statistically significant.

3. Results

3.1. LPA induces ITGB6 mRNA and protein expression in OSCC

To investigate whether LPA induces ITGB6 expression in OSCC cells, SAS and HSC-3 cells were first exposed to different concentrations of LPA for 2 h, and *ITGB6* mRNA levels were measured by qRT-PCR. As shown in Fig. 1A, LPA induced *ITGB6* mRNA expression in a dose-dependent manner, with the maximum increase observed following treatment with 10 μM LPA in both cell lines. Next, time-course experiments with LPA at a concentration of 10 μM showed that *ITGB6* mRNA (Fig. 1B) and protein (Fig. 1C) levels changed over time, with

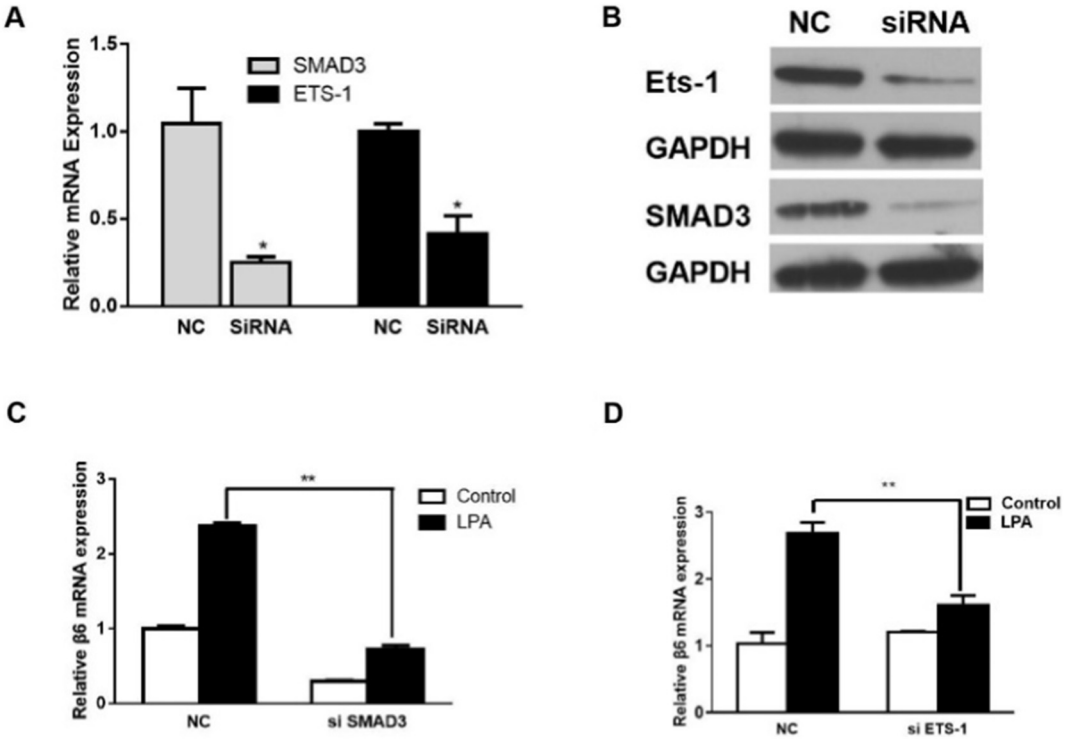

Fig. 3. SMAD3 and ETS-1 are involved in LPA-induced *ITGB6* mRNA expression in OSCC cells. (A&B) Effect of siRNAs on *SMAD3* and *ETS-1* expression. SAS cells were transfected with 100 pM of siRNA against *SMAD3*, *ETS1*, or a scrambled siRNA (negative control, NC) for 48 h. *SMAD3* and *ETS1* mRNA expression was measured by qRT-PCR (A), and protein expression was detected by immunoblotting (B). $*p < 0.05$, compared with the NC group. (C&D) Effect of *SMAD3* and *ETS1* inhibition on LPA-induced *ITGB6* mRNA expression. SAS cells were transfected with (C) SMAD3 siRNA, (D) ETS-1 siRNA, or NC, then cultured in serum-free medium for a further 24 h before the treatment with LPA (10 μM) or media alone (control) for 2 h. The relative expression of *ITGB6* mRNA was determined by qRT-PCR. $**p < 0.01$, compared with the LPA-treated NC group.

the maximal increase observed at 2 h for mRNA and at 4 h for protein. For subsequent experiments, 10 μM LPA was chosen as the preferred dose for studying the mechanism of ITGB6 induction in our cells because this concentration not only induced robust ITGB6 expression but also corresponds to the physiological level of LPA found in serum, which has been estimated to be the range of 2–20 μM LPA [24]. Next, *ITGB6* mRNA stability was assessed using the transcription inhibitor actinomycin D (ActD) [25] to determine whether the effect of LPA on *ITGB6* mRNA levels was due to an enhanced mRNA stabilization. Cells were incubated with ActD (5 μg/ml) alone, or ActD and LPA (10 μM) in combination for 0–20 h. The results showed that LPA had no effect on the decay rate of the *ITGB6* transcripts in either of the two cell lines, indicating that LPA affects *ITGB6* mRNA transcription and not mRNA stability (Fig. 1D).

3.2. Identification of cis-acting elements in the human ITGB6 promoter responsible for LPA-induced ITGB6 transcription

To determine the transcriptional regulation mechanism responsible for the increased *ITGB6* expression induced by LPA, SAS cells were transiently transfected with luciferase reporter constructs containing serial deletions of the human *ITGB6* promoter [pGL2-B6(−3/+208); pGL2-B6(−150/+208); pGL2-B6(−421/+208); pGL2-B6(−908/+208)], and the relative luciferase activity of each construct was analyzed. In order to detect the robust promoter activity driven by LPA, a time-course experiment was performed to find out that there is a maximal increase luciferase activity observed at 8 h after LPA (10 μm) treatment (Data no shown), this time point was then chosen to examine the promoter activity in our subsequent experiments. Compared to the control, LPA significantly upregulated the activity of the constructs pGL2-B6(−150/+208), pGL2-B6(−421/+208), and pGL2-B6(−908/+208), while it had no effect on the activity of pGL2-B6(−3/+208) (Fig. 2A). These results indicate that the C/EBP binding site located between positions −207 and −202, the AP-1 element located between positions −197 and −189, and the STAT3 element located between positions −176 and −169 are not involved in LPA-induced *ITGB6* transcription in SAS cells, whereas the promoter region situated between positions −150 to −3 is essential.

To identify the regulatory elements involved in LPA-induced *ITGB6* transcription in the above region, sequence analysis was performed using TRANSFAC-TESS and Alibaba 2.0 analysis software. Fig. 2B shows that this region contains putative binding sites for the transcription factors ETS-1 and SMAD3. The use of reporter constructs with mutations in the putative binding sites showed that mutations in either of the two binding sites results in 50% inhibition of the *ITGB6* promoter activity induced by LPA, while the simultaneous mutation of both binding sites completely prevented LPA-mediated induction (Fig. 2C). These data suggest that SMAD3 and ETS-1 binding sites are essential for LPA-induced *ITGB6* transcription.

3.3. SMAD3 and ETS-1 are involved in LPA-induced ITGB6 transcription

Next, the role of SMAD3 and ETS-1 on LPA-induced *ITGB6* transcription was assessed in SAS cells by RNAi of *SMAD3* and *ETS-1* using specific siRNAs. Gene knockdown at the mRNA and protein levels was verified by qRT-PCR and western blotting for both ETS-1 and SMAD3 (Fig. 3A and B, respectively). RNAi of either *SMAD3* (Fig. 3C) or *ETS-1* (Fig. 3D) significantly reduced LPA-induced *ITGB6* mRNA levels, indicating that both transcription factors are involved in this LPA-mediated signaling pathway.

To further understand how LPA induces *ITGB6* expression through SMAD3 and ETS-1, activation of these two transcription factors was analyzed in the presence of LPA in SAS cells by western blot. The results showed that LPA treatment increases SMAD3 (Fig. 4A & B) and ETS-1

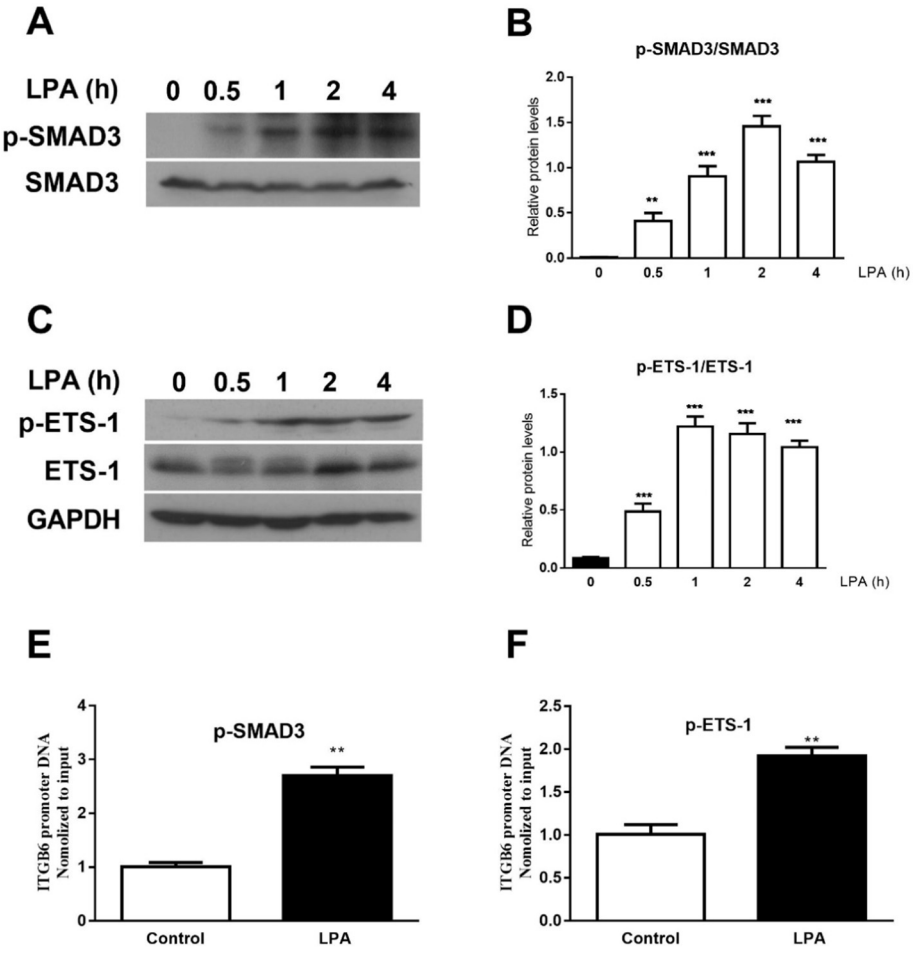

Fig. 4. LPA induces SMAD3 and ETS-1 phosphorylation and binding to the ITGB6 promoter in OSCC cells. (A–C) Analysis of (A) SMAD3 and (C) ETS-1 phosphorylation in SAS cells. Confluent and serum-starved SAS cells were stimulated with LPA (10 μM) for the indicated times, and whole cell extracts were prepared for western blot analysis against p-SMAD3, SMAD3, p-ETS-1, ETS-1, and GAPDH (loading control). Data are representative of three independent experiments. (B–D) The graph shows densitometric analysis of the optical density-based data in the immunoblots shown in Fig. 4A–C. Data are presented as the mean ± SD of three independent experiments. $^{***}p < 0.001$, compared to unstimulated cells. (*E*-F) Measurement of p-SMAD3 and p-ETS-1 binding to the ITGB6 promoter. SAS cells were treated with LPA or media alone for 1 h, and binding of p-SMAD3 (E) and p-ETS-1 (F) to the ITGB6 promoter was detected by ChIP assay. The associated ITGB6 promoter DNA was measured by qPCR. The results are normalized to the input control. Data represent mean ± SEM of triplicates. $^{**}p < 0.01$, compared to the medium control.

(Fig. 4C &D) phosphorylation after 0.5 h treatment, and the activation levels peaked at 2 h or 1 h, respectively. In addition, the in vivo association of these transcription factors with the *ITGB6* promoter was evaluated by ChIP assay after LPA treatment, showing that LPA significantly increased binding of p-SMAD3 (Fig. 4E) and p-ETS-1 (Fig. 4F) to the *ITGB6* promoter.

In summary, these results indicate that the transcription factors SMAD3 and ETS-1 are involved in the induction of human *ITGB6* mRNA expression by LPA in OSCC cells.

3.4. LPAR1 mediate LPA-induced ITGB6 transcription via activation of SMAD3 and ETS-1

There are currently six known LPA receptors that can mediate LPA signaling. To investigate which LPA receptor is responsible for the effect of LPA on ITGB6 transcription, expression of all six LPA receptors was first measured in SAS and HSC-3 cells by qRT-PCR. We found that SAS and HSC-3 cells are mainly expressed LPAR1, LPAR2, and LPAR3, whereas LPAR4, LPAR5 and LPAR6 are lowly expressed. (Fig. 5A). In addition, antibodies against LPAR4, LPAR5 and LPAR6 did not show adequate specificity in our cells. We then focus on LPAR1–3 in our study. Since Ki16425 is a well-known antagonist of both LPAR1 and LPAR3 at concentrations below1 μM [26]. We next used 1 μM Ki16425 [26] to determine which LPA receptors are involved in LPA-induced ITGB6 transcription. We found that 1 μM Ki16425 significantly attenuated LPA-induced ITGB6 mRNA expression (Fig. 5B) and protein production (Fig. 5C) in SAS cells. Furthermore, similar inhibitory effects of Ki16425 on LPA-induced phosphorylation of SMAD3 (Fig. 5D) and ETS-1 (Fig. 5E) were observed. These results suggest that LPA-dependent stimulation of ITGB6 expression may involve LPAR1 and LPAR3 with varying degrees of efficacy.

Next, we used RNA interference to establish the individual contributions of LPAR1and LPAR3 to LPA-induced *ITGB6* transcription. LPAR1- and LPAR3-specific siRNAs [27] successfully silenced LPAR1 and LPAR3 gene expression in SAS cells at the mRNA and protein levels (Fig. 6A–E). Moreover, transfection with LPAR1 siRNA resulted in a significant reduction in LPA-induced ITGB6 mRNA expression (Fig. 6F), while LPAR3 siRNA had no effect (Fig. 6G). These results suggest that LPAR1 is involved in the regulation of LPA-induced ITGB6 expression.

3.5. $G\alpha_i$ is involved in LPA-induced ITGB6 expression in OSCC cells

To determine the signaling pathways by which LPA induced *ITGB6* expression in OSCC cells, the effects of pharmacological inhibitor-PTX was used to block the common LPA signaling cascades on the LPA-induced gene expression. We found that $G\alpha_i$-inhibitor PTX had no significant cytotoxicity (Fig. 7A) but exhibited a dramatic inhibitory effect on LPA-induced *ITGB6* expression at the mRNA (Fig. 7B) and protein levels (Fig. 7C), as well as LPA-induced SMAD3 (Fig. 7D) and ETS-1 (Fig. 7E) phosphorylation. These results indicate that $G\alpha_i$ mediates the effect of LPA via activation of SMAD3 and ETS-1 in SAS cells.

4. Discussion

In the present study, we investigated the role of LPA, an endogenous signal present in tumor environments, on *ITGB6* expression in OSCC cells. We show that LPA induces *ITGB6* expression in OSCC cells at the transcriptional level. Furthermore, we demonstrate that the molecular mechanism mediating LPA-induced *ITGB6* transcription involves coupling of LPAR1 to $G\alpha_i$, and downstream activation of the transcription

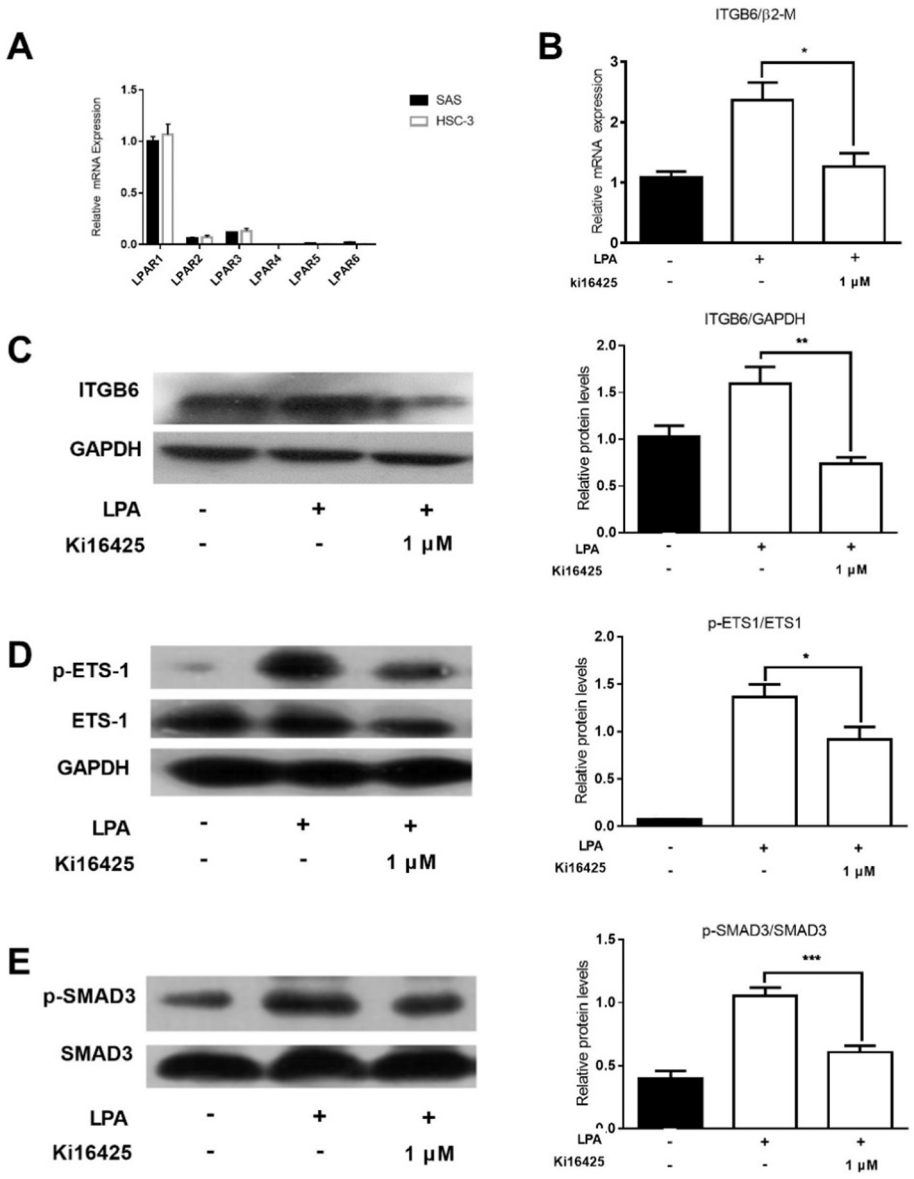

Fig. 5. Ki16425 attenuated LPA-induced *ITGB6* expression and phosphorylation of SMAD3 and ETS-1 in OSCC cells. (A) Real-time qRT-PCR was performed to detect the expression of LPAR1-6 in SAS cells and HSC-3 cells. (B) Effect of Ki16425 on ITGB6 mRNA expression. SAS cells were exposed to LPA (10 μM) for 2 h with or without pre-incubated with Ki16425 (1 μM) for 0.5 h. Final concentrations of DMSO were kept constant for all treatment conditions. ITGB6 mRNA levels were determined by qRT-PCR. $*p < 0.05$, compared with LPA alone. (C-E) Effect of Ki16425 on LPA-induced expression of ITGB6 (c) and phosphorylation of ETS-1 (D) and SMAD3 (E). SAS cells were exposed to LPA (10 μM) for 4 h with or without pre-incubated with 1 μM Ki16425 for 0.5 h. Final concentrations of DMSO were kept constant for all treatment conditions. ITGB6, p-SMAD3, SMAD3, p-ETS-1, ETS-1, and GAPDH (loading control) protein levels were measured by western blotting using specific antibodies. Blots are representative of three independent experiments with similar results. Densitometric analysis was used to quantitatively analyze protein bands. $*p < 0.05$, $**p < 0.01$ compared with LPA alone.

factors SMAD3 and ETS-1 that eventually bind to the *ITGB6* promoter.

LPA has been previously shown to regulate the expression of various genes [14], including those encoding VEGF, interleukin-13, early growth response 1 (EGR1), and COX2. Here, we demonstrate for the first time that LPA can also induce *ITGB6* expression at the protein and mRNA levels in OSCC cells, which is consistent with our previous studies showing that LPA can upregulate *ITGB6* expression in normal human bronchial epithelial cells [28]. These results suggest that LPA may be an organ-independent agonist regulating *ITGB6* expression in cells of epithelial origin. Since *ITGB6* upregulation has been detected in OSCC tissue samples and has been shown to promote OSCC invasion [6,9], it is possible that LPA contributes to OSCC disease progression, at least in part, by upregulating *ITGB6* expression.

LPA signals mainly via LPA receptors of which six types have been described so far. Here, using a specific inhibitor ki16425 and siRNAs against *LPAR1* and *LPAR3*, we found that LPAR1 is the major receptor involved in LPA-induced *ITGB6* transcription in OSCC cells. LPAR1 was the first LPA receptor identified and it is the best characterized [29]. It shows a wide tissue distribution and is aberrantly expressed in several types of cancer cells [30]. LPAR1 signaling has been found to promote invasion and metastasis of cancer cells in breast cancer, ovarian cancer, and pancreatic cancer [31]. The involvement of LPAR1 in upregulation of *ITGB6* expression in OSCC cells, which has been related to OSCC invasion and metastasis, suggests that LPAR1 signaling may also contribute to promote cell malignancy in OSCC.

LPAR1 is a GPCR that couples to the heterotrimeric G proteins $G\alpha_i$, G_q, and $G_{12/13}$ to mediate downstream effects. Here, we show that the $G\alpha_i$-inhibitor PTX significantly abolishes LPA-induced *ITGB6* expression, both at the mRNA and protein levels, and inhibits SMAD3 and ETS-1 phosphorylation, indicating that $G\alpha_i$ mediates LPA signaling to stimulate *ITGB6* expression. These data are in agreement with previous studies showing that LPAR1 couples to $G\alpha_i$ to trigger downstream effects such as upregulate Mcl-1 expression in H19-7 cells [32]. However, to the best of our knowledge, activation of SMAD3 and ETS-1 by LPAR1 coupling to $G\alpha_i$ had not been previously reported extending the downstream effects of this signaling pathway and suggesting that it may mediate LPA signaling in carcinogenesis.

Our previous work demonstrated that LPA induces ITGB6-mediated TGF-β activation, and that TGF-β1 induces *ITGB6* transcription in OSCC cells. We therefore hypothesized that LPA-induced *ITGB6* expression would be mediated by TGF-β1 activation. However, the TGF-β receptor inhibitor LY2109761 does not block LPA-induced ITGB6 protein expression (Supplementary Fig. S1). This suggests that LPA-induced *ITGB6* expression is independent of TGF-β activation signaling, which is

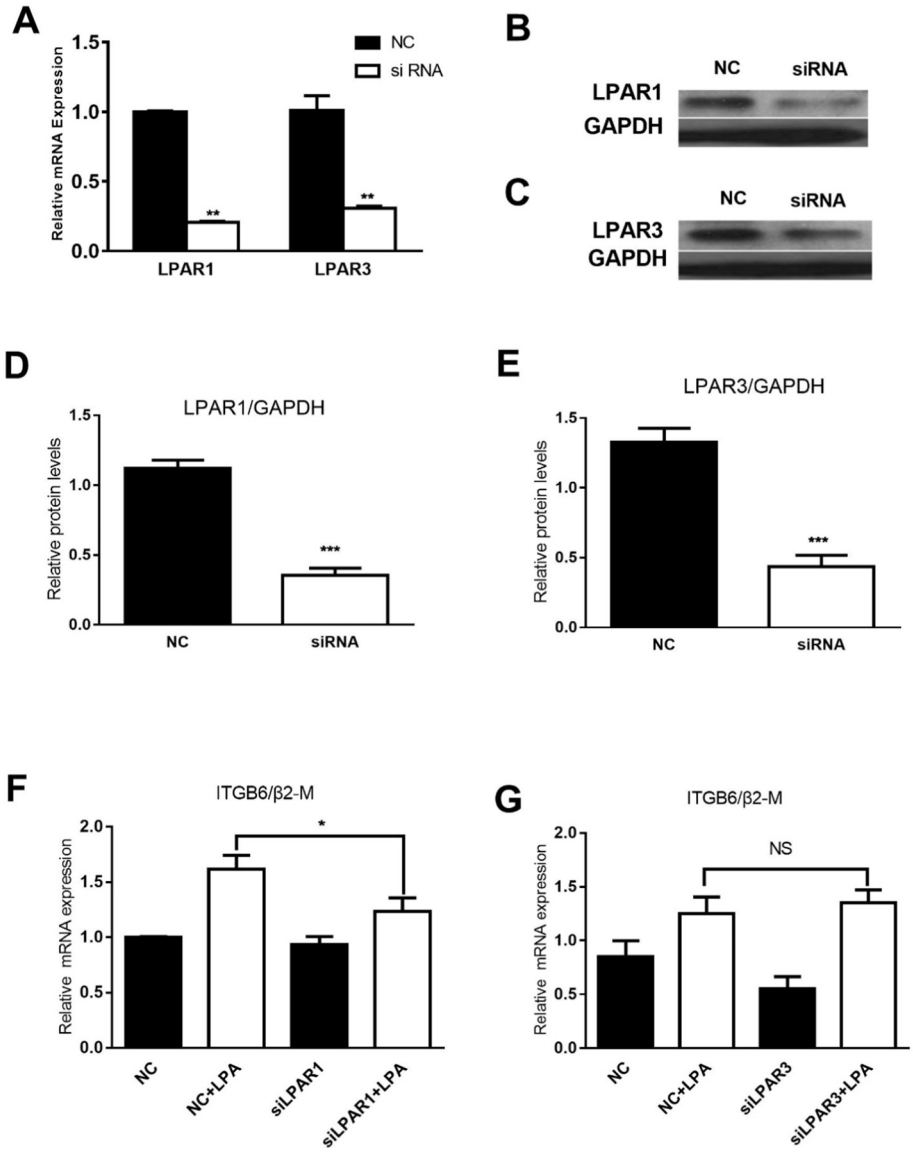

Fig. 6. Effect of LPAR silencing on LPA-induced *ITGB6* expression. SAS cells were transfected with 100 pM siRNA against LPAR1 or LPAR3 or a control siRNA (NC) for 48 h. LPAR1 and LPAR3 mRNA expression was measured by qRT-PCR (A). $^{**}p < 0.01$, compared with the NC group. Protein expression was measured by immunoblotting (B—C). (D-E) The graph shows densitometric analysis of the optical density-based data in the immunoblots shown in B—C. Data are presented as the mean ± SD of three independent experiments. $^{**}p < 0.01$, compared with the NC group. (F-G) Effect of LPAR3 and LPAR1 inhibition on LPA-induced ITGB6 mRNA expression. SAS cells were transfected with LPAR1 siRNA (F), LPAR3 siRNA (G), or NC for 48 h followed by treatment with LPA (10 μM) or medium only, and LPAR1, LPAR3, and ITGB6 mRNA levels were examined by qRT-PCR. $^{*}p < 0.05$, compared with the LPA-treated NC group.

consistent with our previous finding in NHBE cells [28]. Our previous work have also demonstrated that LPA induces integrin β6-mediated TGF-β activation via LPAR2 and $G\alpha_q$ [20]. It would appear, therefore, that LPAR2 may be responsible for coupling to $G\alpha_q$, leading to αvβ6 integrin-mediated TGF-β activation, whereas LPAR1 may preferentially signal via $G\alpha_i$, involved in LPA-induced *ITGB6* expression, for promoting cell invasion and metastasis in OSCC.

ITGB6 transcription is primarily controlled at the transcription initiation level by binding of activated transcription factors to recognition sequences in the gene promoter. Using promoter reporter gene assays, site mutation analysis, siRNAs, and ChIP assay we found that binding of SMAD3 and ETS-1 to the *ITGB6* promoter is critical for *ITGB6* transcription to occur after LPA stimulation in SAS cells. In contrast, we had previously shown that STAT3 and C/EBPα are the major transcription factors regulating the basal expression of *ITGB6* in SAS cells [10], suggesting that different regulatory elements are required for *ITGB6* expression regulation in basal conditions and after LPA stimulation.

The transcription factor SMAD3 is a key molecule in the TGF-β signaling cascade and plays a crucial role in many cancers, including OSCC [33]. The identification and functional characterization of SMAD3 in our study are consistent with a previous report that demonstrated that SMAD3 is responsible for TGF-β1-induced *ITGB6* expression in bile duct epithelial cells [13]. However, how SMAD3 regulates *ITGB6* transcription was previously unclear. Our data provide the first experimental evidence that SMAD3 associates with the *ITGB6* gene promoter in OSCC cells to regulate *ITGB6* expression induced by LPA. These data also suggest that SMAD3 may be an organ-independent transcription factor involved in the transcriptional activation of *ITGB6* in cells of epithelial origin. It was reported that JNK pathway mediated SMAD3 phosphorylation is involved in LPA-induced connective tissue growth factor expression in human gingival fibroblast [34], however, whether JNK pathway is also involved in LPA-induced SMAD3 phosphorylation for regulating *ITGB6* transcription in OSCC cells remains further investigation.

In addition to SMAD3, the transcription factor ETS-1 is also involved in LPA-induced *ITGB6* transcription. ETS-1 is a proto-oncoprotein that belongs to the E26 transformation-specific sequence (ETS) family of transcription factors, which recognize the GGAA/T core motif in target gene promoters [35]. Increased expression of ETS-1 is associated with tumorigenesis in solid tumors [36,37], including betel and tobacco-related oral cancer [38]. The target genes of ETS-1 include receptor tyrosine kinases, matrix metalloproteinases, cell adhesion molecules, and proteins involved in energy metabolism in cancer cells [37]. The identification and functional characterization of ETS-1 in our study are

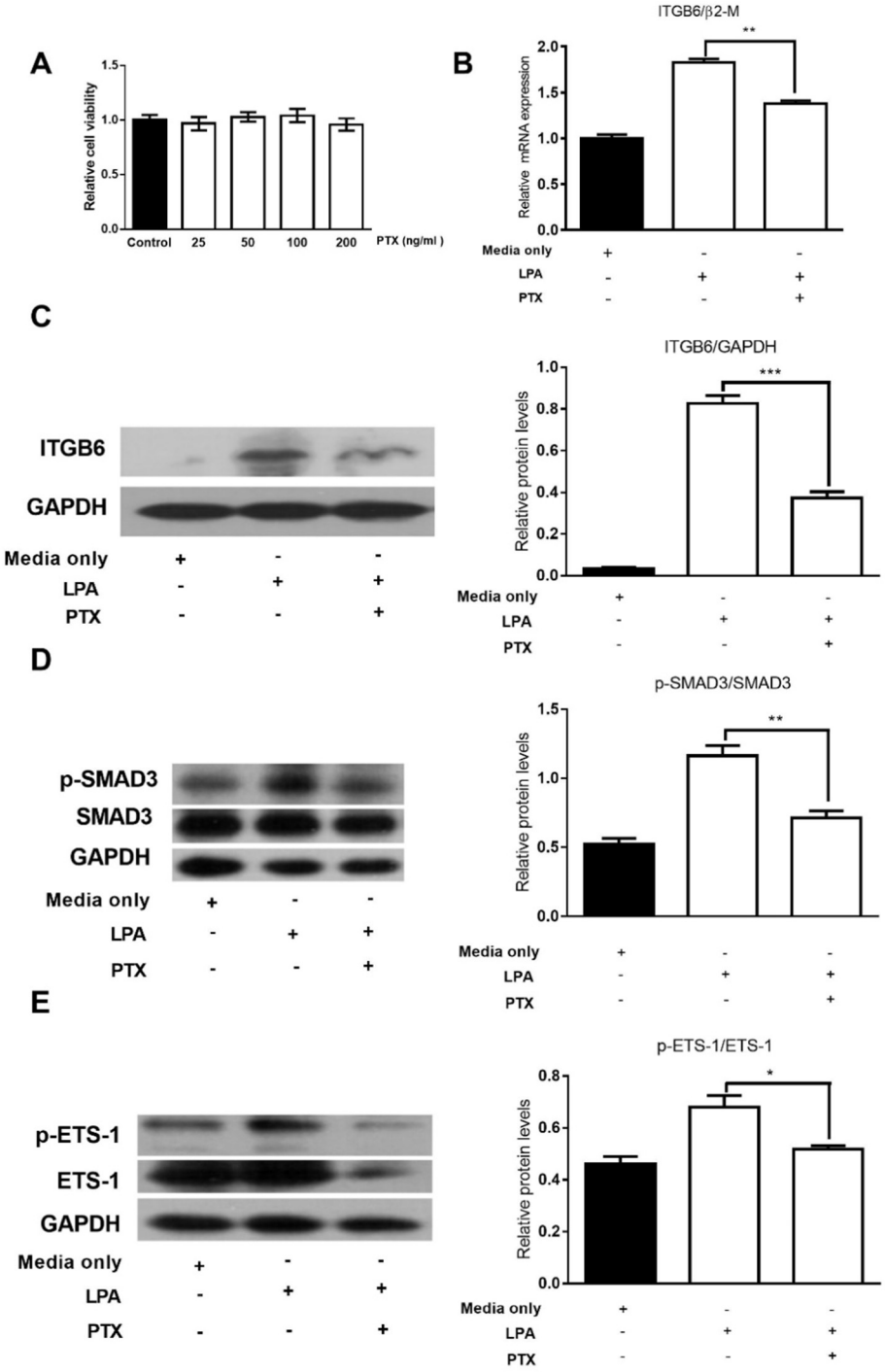

Fig. 7. $G\alpha_i$ is involved in LPA-induced *ITGB6* expression via activation of SMAD3 and ETS-1 in OSCC cells. (A) Effect of the $G\alpha_i$ inhibitor PTX on cell viability of SAS cells. Serum-deprived confluent cells were incubated with different concentrations of PTX for 0.5 h and then assessed by CCK-8 assay. Data are presented as the mean ± SD of three independent experiments. (B) Effect of PTX on ITGB6 mRNA expression. SAS cells were pre-incubated with PTX (100 ng/ml) for 0.5 h, followed by LPA stimulation for 2 h. ITGB6 mRNA levels were determined by qRT-PCR. $^{**}p < .01$, compared with LPA alone. (C-E) Effect of PTX on LPA-induced expression of ITGB6 and phosphorylation of SMAD3, and ETS-1. SAS cells were pre-incubated with PTX (100 ng/ml) for 0.5 h, followed by LPA stimulation for 4 h. ITGB6, p-SMAD3, SMAD3, p-ETS-1, ETS-1, and GAPDH (loading control) were detected by western blotting using specific antibodies. The blots are representative of three independent experiments with similar results. Densitometric analysis was used to quantitatively analyze protein bands. $^{*}p < 0.05$, $^{**}p < 0.01$, $^{***}p < 0.001$ compared with LPA alone.

consistent with a previous report that demonstrated that ETS-1 participates in the transcriptional activation of *ITGB6* in HEK293 cells [12]. However, the role of ETS-1 in the transcriptional activation of *ITGB6* under disease conditions remains unclear. Our data provide the first experimental evidence that LPA activates ETS-1 phosphorylation in oral cancer cells and that phosphorylated ETS-1 binds to the *ITGB6* gene promoter to regulate *ITGB6* transcription in oral cancer cells. It was reported that PI3K-AKT pathway is involved in LPA induced ETS-1 expression in ovarian cancer cells [39], however, whether PI3K-AKT pathway is also involved in LPA-induced ETS-1 phosphorylation for regulating *ITGB6* transcription in OSCC cells remains unclear.

5. Conclusion

Lysophosphatidic acid (LPA) is a lipid growth factor known to regulate diverse cell functions, which contributes to cancer cell migration and invasiveness. We demonstrated that LPA regulates *ITGB6* expression via a transcriptional mechanism in OSCC cells. We propose a model (Fig. 8) in which LPA stimulates *ITGB6* expression via LPAR1 coupling to $G\alpha_i$ and the downstream activation of SMAD3 and ETS-1, which increases their binding affinity to the ITGB6 promoter. Our study provides a cell model for further investigation of the molecular mechanism of *ITGB6* upregulation in OSCC. Clarification of this mechanism in oral carcinomas may have important implications for the future design of therapeutic strategies in the context of cancer invasion

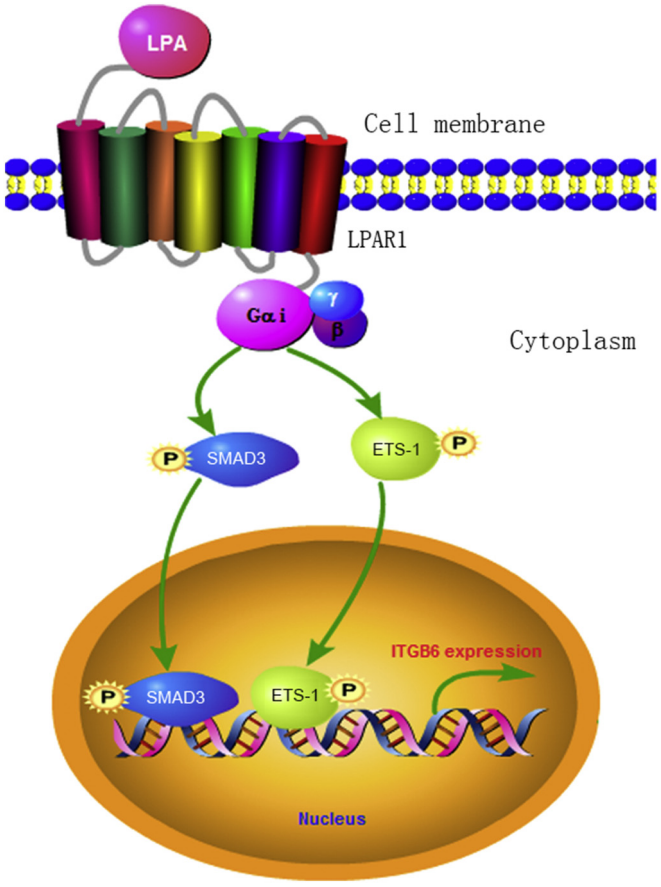

Fig. 8. Schematic diagram of the molecular mechanism driving LPA-induced ITGB6 expression in human OSCC cells. LPA ligation to LPAR1 stimulates Gαi, which leads to increased expression and binding of p-SMAD3 and p-ETS-1 to the ITGB6 promoter, resulting in upregulation of ITGB6 expression.

and metastasis and may provide novel strategies for oral cancer diagnosis and prognosis.

Declaration if interest

The authors report no conflicts of interest in this work.

Author contributions

M.Y.Xu and H. Yin contributed to data acquisition, analysis, and interpretation, drafted and critically revised the manuscript; Y.H.Cai contributed to data acquisition, analysis, and interpretation the manuscript; Q. Ji, W.X. Huang, F. Liu, S.L. Shi, contributed to conception and design, critically revised the manuscript; M.Y.Xu and X.L.Deng, contributed to conception and design, drafted the manuscript. All authors gave final approval and agree to be accountable for all aspects of the work.

Funding

This work was supported by National Natural Science Foundation of China (81671001 and 81072208 to M.Y. Xu, 81771079 and 81370160 to X.L. Deng); the Fundamental Research Funds for the Central Universities (Xiamen University, No. 20720160053 to X.L. Deng); Fujian Province Science Foundation for Youths (No. 2015J05171 to X.L. Deng); Training project of young talents in health system of Fujian Province (2015-ZQN-ZD-35 to M.Y. Xu); Science and technology projects of Xiamen Medical College (K2016-39); and Joint research projects for major and critical diseases of Xiamen City (3502Z20179051 to W.X. Huang and X.L. Deng). The authors declare no potential conflicts of interest with respect to the authorship and/or publication of this article.

Acknowledgments

The authors sincerely thank Professor Yucai Fu (Shantou University Medical College, China) for their kind assistance during the preparation of this manuscript.

Appendix A. Supplementary data

Supplementary data to this article can be found online at https://doi.org/10.1016/j.cellsig.2019.04.008.

References

[1] L.A. Torre, F. Bray, R.L. Siegel, J. Ferlay, J. Lortet-Tieulent, A. Jemal, CA Cancer J. Clin. 65 (2015) 87–108.
[2] C. Scully, J. Bagan, Oral Oncol. 45 (2009) 301–308.
[3] T. Yoshii, Y. Geng, S. Peyton, A.M. Mercurio, V.M. Rotello, Drug Discov. Today 21 (2016) 1489–1494.
[4] R.O. Hynes, Cell 110 (2002) 673–687.
[5] C. Kim, F. Ye, M.H. Ginsberg, Annu. Rev. Cell Dev. Biol. 27 (2011) 321–345.
[6] G.J. Thomas, M.L. Nystrom, J.F. Marshall, J. Oral Pathol. Med. 35 (2006) 1–10.
[7] A. Bandyopadhyay, S. Raghavan, Curr. Drug Targets 10 (2009) 645–652.
[8] D.M. Ramos, D.M. Dang, S. Sadler, Anticancer Res. 29 (2009) 125–130.
[9] H.X. Li, J.H. Zheng, H.X. Fan, H.P. Li, Z.X. Gao, D. Chen, J. Oral Pathol. Med. 42 (2013) 547–556.
[10] M. Xu, X. Chen, H. Yin, L. Yin, F. Liu, Y. Fu, J. Yao, X. Deng, PLoS ONE 10 (2015) e0121439.
[11] M. Xu, L. Yin, Y. Cai, Q. Hu, J. Huang, Q. Ji, Y. Hu, W. Huang, F. Liu, S. Shi, X. Deng, J. Cell. Biochem. 119 (2018) 4193–4204.
[12] R.C. Bates, D.I. Bellovin, C. Brown, E. Maynard, B.Y. Wu, H. Kawakatsu, D. Sheppard, P. Oettgen, A.M. Mercurio, J. Clin. Investig. 115 (2005) 339–347.
[13] B.P. Sullivan, K.M. Kassel, S. Manley, A.K. Baker, J.P. Luyendyk, J. Pharmacol. Exp. Ther. 337 (2011) 471–478.
[14] G.B. Mills, W.H. Moolenaar, Nat. Rev. Cancer 3 (2003) 582–591.
[15] Y. Xu, Z.Z. Shen, D.W. Wiper, M.Z. Wu, R.E. Morton, P. Elson, A.W. Kennedy, J. Belinson, M. Markman, G. Casey, JAMA J. Am. Med. Assoc. 280 (1998) 719–723.
[16] S.P. Bathena, J. Huang, M.E. Nunn, T. Miyamoto, L.C. Parrish, M.S. Lang, T.P. McVaney, M.L. Toews, D.R. Cerutis, Y. Alnouti, J. Pharm. Biomed. Anal. 56 (2011) 402–407.
[17] I.J. Brusevold, I.H. Tveteraas, M. Aasrum, J. Odegard, D.L. Sandnes, T. Christoffersen, BMC Cancer 14 (2014) 432.
[18] A. Gschwind, N. Prenzel, A. Ullrich, Cancer Res. 62 (2002) 6329–6336.
[19] Y. Kihara, H. Mizuno, J. Chun, Exp. Cell Res. 333 (2015) 171–177.
[20] M.Y. Xu, J. Porte, A.J. Knox, P.H. Weinreb, T.M. Maher, S.M. Violette, R.J. McAnulty, D. Sheppard, G. Jenkins, Am. J. Pathol. 174 (2009) 1264–1279.
[21] E.M. Duran, P. Shapshak, J. Worley, A. Minagar, F. Ziegler, S. Haliko, I. Moleon-Borodowsky, P.A. Haslett, Front. Biosci. 10 (2005) 2955–2965.
[22] K.L. Heckman, L.R. Pease, Nat. Protoc. 2 (2007) 924–932.
[23] J.A. Dahl, P. Collas, Nat. Protoc. 3 (2008) 1032–1045.
[24] J. Aoki, A. Taira, Y. Takanezawa, Y. Kishi, K. Hama, T. Kishimoto, K. Mizuno, K. Saku, R. Taguchi, H. Arai, J. Biol. Chem. 277 (2002) 48737–48744.
[25] R.P. Perry, D.E. Kelley, J. Cell. Physiol. 76 (1970) 127.
[26] H. Ohta, K. Sato, N. Murata, A. Damirin, E. Malchinkhuu, J. Kon, T. Kimura, M. Tobo, Y. Yamazaki, T. Watanabe, M. Yagi, M. Sato, R. Suzuki, H. Murooka, T. Sakai, T. Nishitoba, D.S. Im, H. Nochi, K. Tamoto, H. Tomura, F. Okajima, Mol. Pharmacol. 64 (2003) 994–1005.
[27] M. Yang, W.W. Zhong, N. Srivastava, A. Slavin, J. Yang, T. Hoey, S. An, Proc. Natl. Acad. Sci. U. S. A. 102 (2005) 6027–6032.
[28] X.U. MY, D.E.N.G. XL, X.H. CHEN, L.H. YANG, Y.A.O. XW, F.U. YC, Chin. J. Pathophysiol. 28 (2012) 488–491.
[29] J.W. Choi, D.R. Herr, K. Noguchi, Y.C. Yung, C.W. Lee, T. Mutoh, M.E. Lin, S.T. Teo, K.E. Park, A.N. Mosley, J. Chun, Annu. Rev. Pharmacol. Toxicol. 50 (2010) 157–186.
[30] S. Willier, E. Butt, T.G. Grunewald, Biol. Cell. 105 (2013) 317–333.
[31] T. Tsujiuchi, M. Araki, M. Hirane, Y. Dong, N. Fukushima, Histol. Histopathol. 29 (2014) 313–321.
[32] Y. Sun, J.S. Nam, D.H. Han, N.H. Kim, H.K. Choi, J.K. Lee, H.J. Rhee, S.O. Huh, Cell. Signal. 22 (2010) 484–494.
[33] S. Poomsawat, J. Punyasingh, P. Vejchapipat, Clin. Oral Investig. 19 (2015) 613–618.
[34] C.Y. Wang, Y.T. Deng, S.Y. Huang, C.M. Liu, H.H. Chang, M.Y. Wong, J. Formosan Medical Assoc. Taiwan Yi Zhi 113 (2014) 50–55.
[35] F.O. Bartel, T. Higuchi, D.D. Spyropoulos, Oncogene 19 (2000) 6443–6454.
[36] A. Kar, A. Gutierrez-Hartmann, Crit. Rev. Biochem. Mol. Biol. 48 (2013) 522–543.
[37] G.M. Sizemore, J.R. Pitarresi, S. Balakrishnan, M.C. Ostrowski, Nat. Rev. Cancer 17 (2017) 337–351.
[38] P. Pande, S. Soni, N. Chakravarti, M. Mathur, N. Shukla, R. Ralhan, Cancer Detect. Prev. 25 (2000) 496–501.
[39] U. Ray, S. Roy Chowdhury, M. Vasudevan, K. Bankar, S. Roychoudhury, S.S. Roy, Mol. Oncol. 11 (2017) 491–516.